Characterization of SiO_2-TiO_2 Coatings on 316l Stainless Steel Substrates

Manuel Gutierrez[1], Lizangela Guerra[2], Barbara Bermudez-Reyes [2], Roberto Cabriales[2], Luis Reyes[2*]

[1] Student, Universidad Autónoma de Nuevo León, Facultad de Ingeniería Mecánica y Eléctrica, Centro de Investigación e Innovación en Ingeniería Aeronáutica, N.L., México.

[2] Universidad Autónoma de Nuevo León, Facultad de Ingeniería Mecánica y Eléctrica, Centro de Investigación e Innovación en Ingeniería Aeronáutica, N.L., México.

ARTICLE INFO

Article history:

Received 7 January 2018
Accepted 14 June 2018
Available online 15 June 2018

Keywords:

Nano-indentation
316L stainless steel
Sol- gel
SiO_2-TiO_2

ABSTRACT

This paper reports nano-structured SiO_2-TiO_2 coatings using the sol-gel technique on 316L steel substrates. Nanoindentation, surface analysis and corrosion resistance tests were performed on different samples. The nanomechanical tests allowed to compare the uncoated steel samples (E_{avg} = 193.24GPa and the mean hardness of 2.63GPa and coated steel samples (E_{avg} = 287.38GPa and mean hardness of 5.74GPa), resulting in an improvement of the resistance and modulus of elasticity of the coated steel substrates. From a surface analysis an average thickness of 1.12μm was obtained in the coated samples, presenting a dense and consolidated coating. Polarization resistance (PR) and electrochemical impedance spectroscopy (EIS) tests were performed. The PR tests showed a resistance of 2.11×10^5 (Ω cm^2) for the uncoated steel, while the coated steel showed a resistance of 3.46×10^5 (Ω cm^2), indicating an increase in resistance compared to the bare steel. The EIS tests showed greater resistance by the coated steel (5.8×10^5 (Ω cm^2)) compared with the bare steel (2.8×10^5 (Ω cm^2)). The effects of the electrolyte in both conditions were observed by SEM after immersion for 24 h, showing pitting by the bare steel and good protection by the coated steel.

1-Introduction

Improvement of mechanical properties of steel has made possible its use in a large variety of engineering applications. However, oxidation is a current concern of the modern industry due to the deterioration of metallic components [1]. It is estimated that the annual cost of corrosion exceeds 3% of world GDP where a saving of 20 to 25% of this cost can be obtained through the application of corrosion control technologies [2]. There is a great investment in the development of stronger protective coatings in order to reduce the effects of corrosion [3]. For a long time, corrosion protection systems have been sought to guarantee longer protection times and at the same time improve the mechanical strength of structures. One of the main protection systems is the SiO_2 and TiO_2 coating developed by the sol-gel method. These coatings offer very interesting properties and provide improvements in chemical and mechanical properties. Thin films of TiO_2 are used in a wide range of applications, such as ultraviolet filters for optics and packaging materials, anti-

* Corresponding author:
E-mail address: luis.reyessr@uanl.edu.mx

reflective coatings for photovoltaic cells, passive solar collectors, and many more applications. Several techniques have been developed for the preparation of thin films of TiO_2, including sputtering deposition, laser deposition, and sol-gel techniques. The sol-gel techniques have advantages over other procedures due to the excellent control over the composition, homogeneity due to the mixture of liquid precursors, and lower crystallization temperatures [4-7].

Ceramic SiO_2-TiO_2 coatings are attractive due to resistance against corrosion of steel, in addition to their application in photocatalysis and self-cleaning. SiO_2-TiO_2 nanocomposites are used as glass materials presenting extremely low thermal expansion coefficients and high levels of refraction. The advantages of these coatings include corrosion protection, high thermal stability, excellent mechanical strength (as a property of SiO_2), chemical stability and higher coefficient of thermal expansion (as property of TiO_2) [8]. Ceramic coatings have recently been studied for their corrosion protection characteristics. The most commonly oxides used as coatings are: SiO_2, TiO_2, Al_2O_3 and ZrO, being deposited on different metallic substrates such as steels, Al and Ti. The main difficulty found in the development of sol-gel coatings is the formation of cracks that can induce coating failures. In previous works, Shayegh [8] reported an improvement in the corrosion resistance of 316L steel, low roughness and good photo-cathode protection. Gobra [9] used nanoparticles of TiO_2 and SiO_2 which were introduced into hybrid silica sol-gel/epoxy coating to enhance the mechanical properties of coatings. This coating was applied to 3003 aluminum alloy surface, and the results showed a significant improvement of the adhesion performance of hybrid silica sol gel coating due to the addition of TiO_2. Also, the hydrophobicity of sol-gel coating increased due to the addition of SiO_2 nanoparticles. Apart from its excellent properties in corrosive atmospheres, SiO_2-TiO_2 coatings are used in biomedical applications. In a work developed by Mendoza [7], the state of the art of applications and properties of SiO_2-TiO_2 coatings is presented. On the other hand, recent advances in mechanical testing techniques at microscale including nano-indentation have made it possible to ascertain properties to sub-micron size or multi-layer structures [10, 11]. With these techniques it is possible to measure the mechanical behavior in diverse coatings.This work aims to acquire knowledge in the improvement of the mechanical and chemical properties of 316L stainless steel substrates, by virtue of its wide application in the automotive sector.

2-Experimental procedure

316L stainless steel specimens of 12 mm diameter and 10 mm height were machined and sectioned. In addition, rectangular 36 mm × 29mm samples were prepared. An OLYMPUS DELTA X-DP 2000 XRF analyzer was used for the determination of chemical composition (wt.%) of 316L steel; Fe 69.21, Cr16.42, Ni 10.15, Mo 2.03, Mn 0.89, Si 0.49, Cu 0.29, Co 0.22, S 0.13, V 0.091, P 0.064 and Nb 0.013. The substrate was characterized using a ZEISS Observer Z1 microscope and a JEOL JSM-6510LV scanning electron microscope in topography, energy-dispersive spectroscopy (EDS) and chemical mapping modes.

The coatings were produced by the sol-gel process. Tetraethoxysilane (TEOS) from Sigma Aldrich and ethanol (EtOH) from Baker were used in a 1: 1 ratio. Subsequently, deionized water and HNO_3 were added as catalyst and 3 wt.% of SiO_2 of TiO_2 nanoparticles were previously functionalized. The mixture was stirred for complete hydrolysis. To deposit the coatings on the 316L substrate, the dip coating technique at a speed of 0.125mm /sec was used. The drying and solvents evaporation was carried out at 180 °C and they were thermally treated for consolidation at 300 °C for 2 h. The surface analysis is based on the value of the average roughness (Ra) measured in microns between the points analyzed. The SiO_2-TiO_2 films were measured on the coated steel plates, and the measurements were obtained based on the step technique acquiring an average thickness. Roughness and thickness measurements of SiO_2-TiO_2 films were performed using a Brucker Contour GT profiler, the profiler measures thickness for every point in the field of view highlighting variations in thickness and uniformity across an area up to 50 mm^2; additionally, the topography of both the film and substrate surface is returned.

Nano-indentation tests were performed in a CSM Instrument 50-191Nanoindentator, and a Berkovich type diamond tip was used and a minimum resolution depth of 0.04μm was selected. The test parameters are shown in Table 1. Nano-indentation was performed in a rectangular pattern of 4 x 5 with a separation of 20μm on the X axis and 30μm on the Y axis. The parameters were selected taking care that the nanoindentant does not exceed more than 20% of the thickness of the coating, avoiding the interference of the substrate. The variation of parameters for the coated and uncoated substrates was due to different mechanical and chemical properties of the protective film. Damages and fractures in the film were observed at higher loads. The parameters were proposed by a series of experiments of several tests along the entire surface.

Table 1. Parameters used in the nano-indentation tests

Parameters	Coated samples	Un-coated samples
Applied load (mN)	10	500
Loading rate (mN/min)	20	700
Deposition time (s)	2	2

Two tests were performed to evaluate corrosion resistance: polarization resistance (PR) and electrochemical impedance spectroscopy (EIS). Polarization resistance is a technique commonly used in material corrosion studies to obtain the corrosion rate data. As the potential of the material (working electrode) is changed, a current will be induced to flow between the working and counter electrodes. The slope between the induced potential and the resulting current is interpreted as the polarization resistance. This resistance can then be used to find the corrosion rate of the material using the Stern-Geary equation.For PR tests, a Solarton SI 1287 equipment was used with 27.9g equivalent weight of 316L steel to obtain a value in mm/year [12, 13].The amplitude of the voltage perturbation was 10 mV. The parameters for polarization resistance were obtained at a constant scan rate of 0.1667 mV/s by sweeping the potential between -0.015 and 0.015 V.

EIS measurements were conducted in Solartron SI 1260 equipment and GAMBRY electrolytic cell in 3 wt.% NaCl after 24h immersion.The EIS tests were performed under a three-electrode system; a 316L steel plate was used as the working electrode, Calomel electrode was used as a reference electrode, and a platinum mesh was used as an auxiliary electrode. The contact area was 1 cm^2 and up to 5 measurements were performed on each sample to ensure reproducibility. The measurements were performed in the frequency range of 10 - 0.001 Hz (5 points were measured for each decade of frequency). The amplitude of the voltage perturbation was 10mV.

3-Result and discusion

Microstructural characteristics of the uncoated 316L stainless steel such as the grain size, twining and precipitates are shown in Fig. 1. The average grain size was measured according to the ASTM E-112 standard by the linear intercept method obtaining an average grain size of 44.9μm. Fig. 2 shows an SEM micrograph of a coated sample at 2000X where a uniform and homogeneous coating without fractures is observed. In addition, some precipitates of the substrate are observed in Fig. 2a.

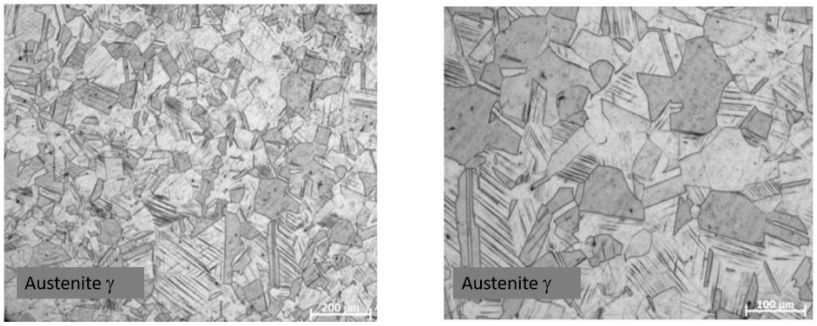

Fig. 1. a) Microstructure of 316L stainless steel at 50X and b) at 100x

Fig. 2b shows the EDS measurements of the coating, it was filtered in such a way that only the main components of the coating and substrate were observed. High contents of Si and O can be observed due to the SiO_2 coating base. Also, a small amount of Ti can be observed due to the TiO_2 nanoparticles in the sol-gel matrix of SiO_2-TiO_2.

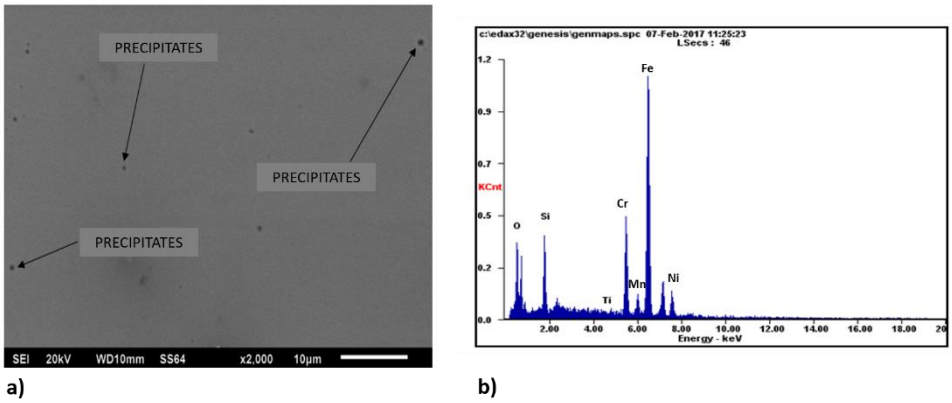

Fig. 2. a) SEM micrograph of a coated sample at 2000X and b)EDS measurementsof SiO_2-TiO_2 coating

A chemical mapping for the coating main elements is observed in Fig. 3. Fig. 3a shows the distribution of O in the selected area, and Fig. 3b shows Si, Fig. 3c shows Ti distribution and Fig. 3d shows the distribution of O, Si and Ti. A uniform distribution of the coating elements with a lower concentration of Ti is observed in the chemical mapping. Table 2 shows the percentages of O, Si and Ti obtained in the chemical mapping. The performed mapping shows that the elements Ti, Si and O are uniformly distributed in the substrate. The morphology and chemical composition analysis shows a homogeneous SiO_2-TiO_2 coating, transparent and without fractures. The surface analysis was performed on the coated samples obtaining a very small roughness and thickness (see Fig. 4). Fig. 4a shows the steel coated presenting an average roughness of 631.5 nm, which was based on the colorimetric scale. Ruíz [14] reported roughness values of about 400 nm for a monolayer of SiO_2-TiO_2 coatings on stainless steel substrates. Krzak [15] reported roughness values from 160 nm to 630 nm for coatings of SiO_2-TiO_2 on 316L steel substrates. However, instead of using TEOS as a precursor, they used as a precursor a combination of TEOS / diethoxydimethylsilane (DEMS). In Fig. 4b an average thickness of 1.12 µm was observed in the coated samples. Previous works reported values from 0.5µm to 3 µm for coatings on 316L stainless steel substrates [16, 17].

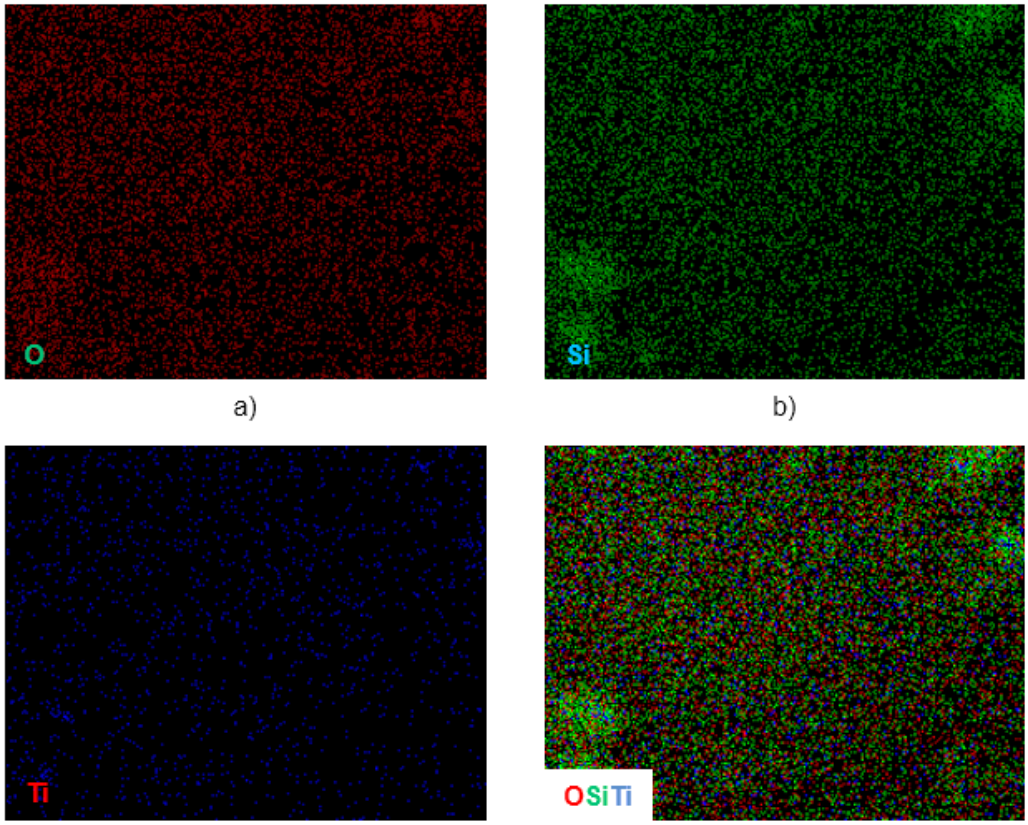

Fig. 3. Chemical mapping of coating elements distribution a) Oxygen, b) Silicon, c) TiO_2 and d) SiO_2-TiO_2

Table 2. Atomic and weight percentage of O, Si and Ti

Element	Weight,%	Atomic,%
OK	65.83	77.71
SiK	31.69	21.31
TiK	02.48	00.98

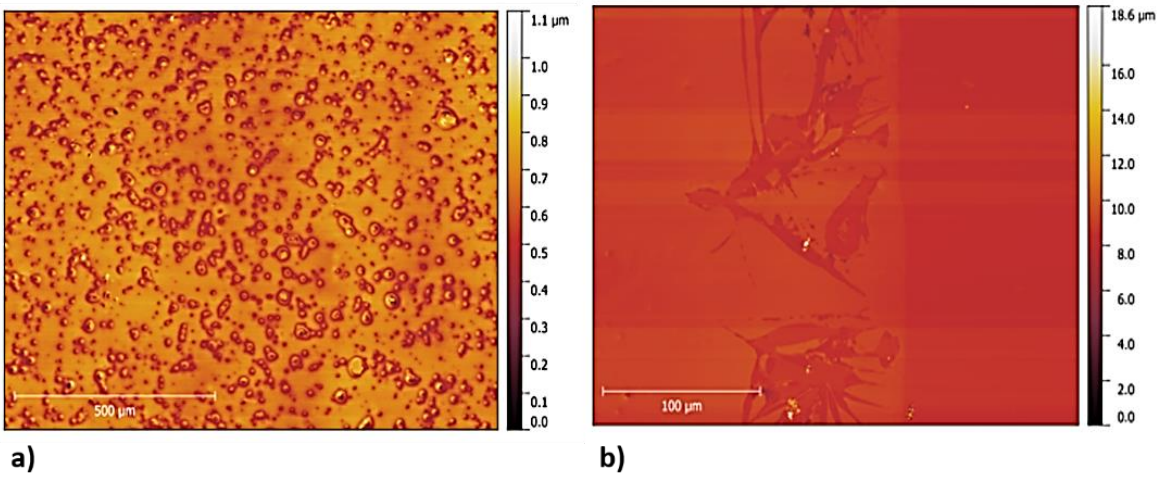

Fig. 4 a) Surface roughness and b) coating thickness of SiO_2-TiO_2 /316L substrate

Nano-indentation tests were performed on the coated and uncoated substrates for obtaining hardness value and elastic modulus. In Fig. 5, the load-displacement graphs are presented, and the graphs show a ductile behavior without stacking in the indentation [18, 19]. Considering that the coating thickness is approximately 1μm, the penetration in the coating was between 100 to 250 nm according to the Oliver and Pharr preventive method which indicates that the penetration depth should be from 10% to 25% of the coating thickness in order to avoid interference of the substrate [19]. It can be seen in the loading and unloading curve of the coating that it has a different behavior. Like the steel, the deformation made by the indentation is plastic-elastic without stacking around the indentation [20].

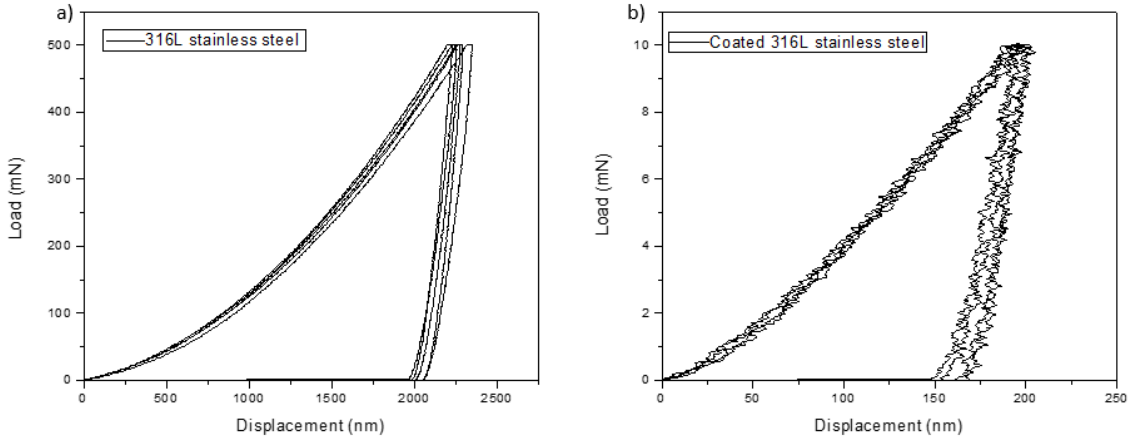

Fig. 5. a) Load-displacement graph of uncoated 316L stainless steel and b) load-displacement graph of coated 316L stainless steel

Table 3 shows the average Young's modulus and hardness value in GPa for the coatings. The steel obtained an average Young's modulus of 193.24 GPa, and an average hardness value of 2.63 GPa, which coincides with the standard steel parameters [21, 22]. While the coating obtained an average Young's modulus of 287.38 GPa and an average hardness value of 5.74 GPa. In accordance with Ohring [23], thin films Young´s module can increase from 60-120%. In this case the SiO_2-TiO_2 coating Young´s Module increased 48.71%.

Table 3. Hardness average value and Young's modulus value of the coated and uncoated samples

Uncoated 316L Stainless steel		Coated 316L Stainless steel	
E (GPa)	HV(GPa)	E (GPa)	HV (GPa)
193.24	2.63	287.38	5.74

To determine the corrosion behavior of 316L stainless steel and SiO_2-TiO_2 coatings, PR and EIS tests were performed. From the PR test it is observed that the average corrosion rate of coated steel is 1.85×10^{-3} mm/year while in the bare steel it was 3.50×10^{-3}mm/year which shows a lower corrosion rate in the coated steel against bare steel. This is reflected in the average corrosion resistance; in the coated steel it is 3.46×10^{5} (Ω cm^2) while in the bare steel it was 2.11×10^{5} (Ω cm^2), showing a greater resistance of coatedsteel against bare steel. The corrosion density was reduced from 3.05×10^{-7} (A cm^2) to 1.61×10^{-7} (A cm^2) for the coated samples. Lower

values indicate better corrosion resistance. The corrosion behavior agrees with literature.

The EIS results of corrosion behavior are shown Figs. 6 and **7.** Nyquist and Bode Plots were analyzed to determine the corrosion rate of SiO_2-TiO_2coatings**.**

From the Nyquist plot, the red line represents the behavior of the coating and the black line represents that of the bare steel. A box is added to observe the behavior at low frequencies. The corrosion rate was determined by the diameter of semicircles which is recognized to be related with the corrosion resistance. Large diameter indicates a low-corrosion rate. Measurements of impedance and phase angle with respect to frequency are plotted in Fig. 7. The phase plot at low and medium frequency shows the load transfer process between the coating/solution interface. The high phase values in these regions are associated with porosity or diffusion processes [24]. It can be seen that in most of the diagram the coated steel is below the uncoated steel which usually indicates little porosity and better resistance. However, the medium frequency area shows high phase values which could be associated with the beginning of porosity or diffusion.

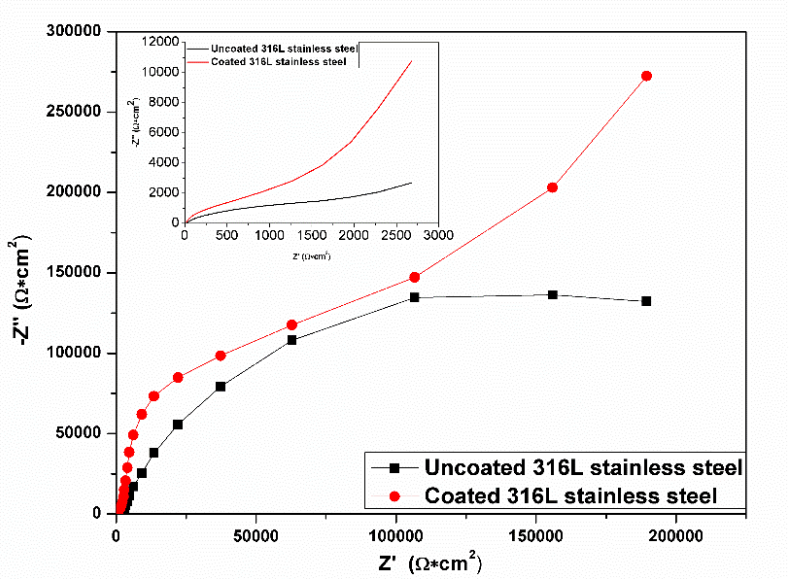

Fig. 6. Nyquist plots for the SiO_2-TiO_2 coated and bare Steel

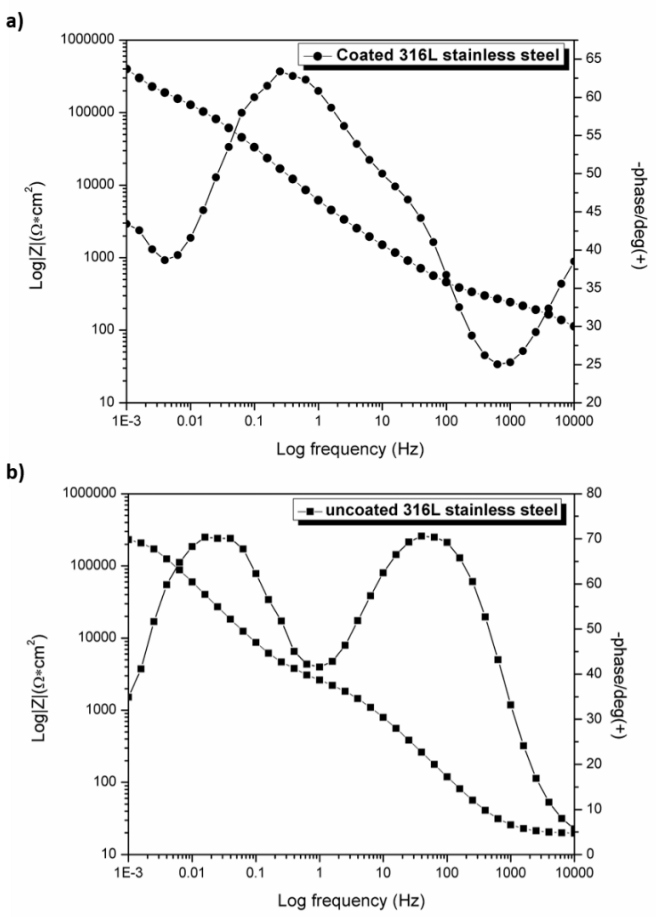

Fig. 7. Bode diagram of coated and uncoated substrates

The influence of the diffusion phenomenon shown at low frequencies indicates the presence of transport species through the metal-substrate interface [25]. The higher Z modulus at lower frequency indicates a better corrosion resistance. The EIS results from the equivalent circuits were applied to describe the electrochemical behavior of the coated and uncoated steel using the curve fitting method (see Figure 8). Fig. 8a shows the circuit used to extract the data from the results of a time constant Bode plot. The circuit consists of a resistor RS, which represents the resistance of the solution, a capacitor C1 and a resistor R1, which are parallel with each other. R1 is the charge transfer resistance of the steel and C1 the pseudocapacitance of double layer formed at the metal solution interface. Fig. 8b shows a resistor RS connected to a resistor R1 and a capacitance C1 or constant phase element, where the constant phase element describes the behavior of the coating formed by the interface of the solution and the metal, the resistors R1 is the resistance of the ionic conduction paths, as the pores and cracks are developed in the coating. In series with the resistance R1 there is a second capacitor C2 and a second resistor R2, where R2 and C2 are the load transfer resistance at the metal/electrolyte interface and pseudocapacitance of double layer, respectively. In order to compare the resistance of the uncoated steel the value of R1 is taken for circuit 1 and the value of R2 is taken for circuit 2 [24]. From circuit 2, a high value of R1 and a low value of C1 indicate that the values of defects and porosity are low. The high values of R2 and the low values of C2 indicate a good resistance to corrosion. The values obtained from the circuits are given in Table 4.

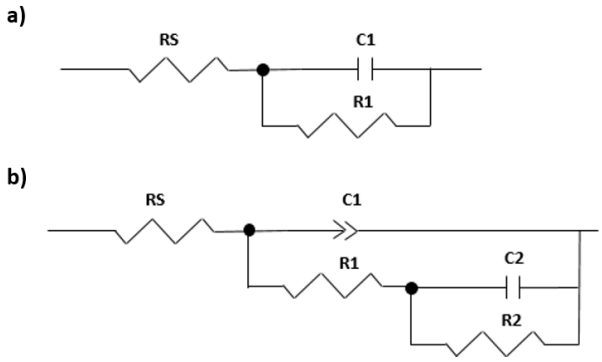

Fig. 8. a) Equivalent circuit on experimental data for uncoated steel and b) coated steel

Table 4. Electrochemical parameters obtained from equivalent circuits

	RS, Ω cm^2	C1, F cm^{-2}	R1, Ω cm^2	R2, Ω cm^2	C2, F cm^{-2}
Un-coated	3.096	3.855×10^{-4}	2.8×10^{5}	-	-
Coated	175.3	4.61×10^{-5}	3.29×10^{5}	5.85×10^{5}	5.55×10^{-4}

From the EIS tests, using equivalent circuits, a 5.8×10^{5} (Ω cm^2) resistance was obtained from the coated steel, while in the bare steel a resistance of 2.8×10^{5} (Ω cm^2) was obtained, showing a clear superiority on the coatings.

The interface between coating and bare steel is shown in Fig. 9. After being immersed for 24 h in NaCl, the bare steel shows imperfections, pitting and concentration of NaCl, while the coated area shows no imperfections and only selective concentration of NaCl. SEM analysis of the pitting was carried out in order to analyze their morphology and the chemical composition of the corrosion remnants through EDS measurements.Fig. 10 shows spherical pitting and chemical analysis performed on the pit. The analysis showed high oxygen content due to the oxide produced in the pitting after 24 h in NaCl. The stainless substrate will be corroded and pitted in the coating cracks due to the expansion coefficient difference between the stainless steel substrate and the coating. But it is also quite possible that fine pores have been formed during the heat treatment of the film. Through these pores electrolyte may penetrate and reach the steel surface leading to its corrosion.

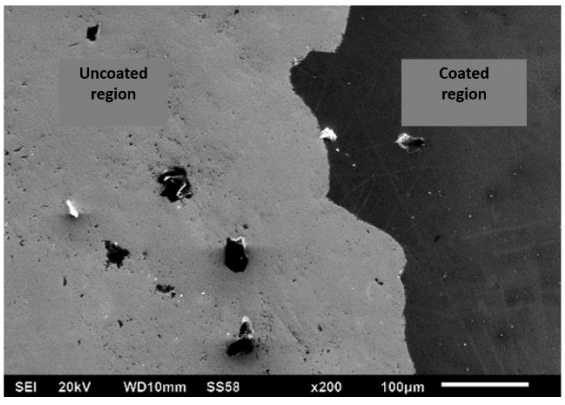

Fig. 9. Micrograph of the coated and bare steel after being immersed for 24 h in NaCl

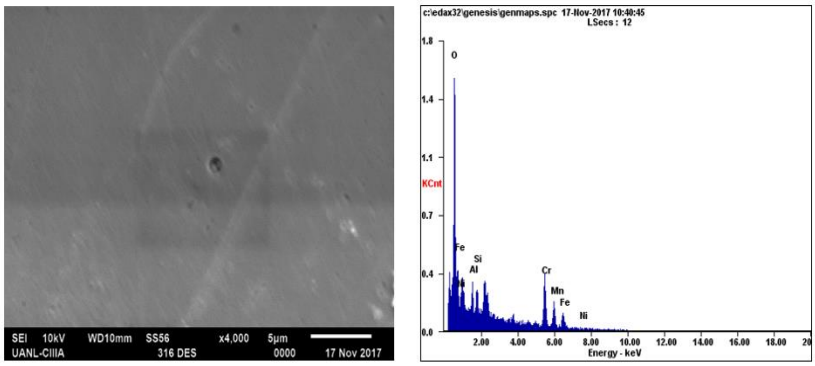

Fig. 10. a) SEM micrograph of pitting in bare steel and b) EDS measurementsof SiO_2-TiO_2 coating on the pitting zone

4-Conclusions

SiO_2-TiO_2 coatings were developed by sol-gel method and dip-coating technique on 316L stainless steel substrates. It was confirmed that the sol-gel technique is a simple and cost-effective method for the preparation of coatings. In addition, it was verified by SEM that the coating is highly transparent, homogeneous, not very rough and does not present fractures. The analysis by x-ray spectroscopy confirmed the presence of the coating on the substrates revealing the existence of TiO_2 nanoparticles. The nano-indentation tests showed that the SiO_2-TiO_2 coatings had an average Young's modulus of 287.38 GPa and a hardness of 5.74GPa; in contrast, the bare steel obtained an elastic modulus of 193.24 GPa and a hardness value of 2.63 GPa. The hardness values of the coated steel showed an increase of 48.71 % in the Young's modulus and an increase of 118 % in the hardness value. It is established that the SiO_2-TiO_2 coatings have a good resistance to corrosion. The PR and EIS tests showed that the SiO_2-TiO_2 coatings achieved an improvement in the corrosion resistance of 3.46×10^5 (Ω cm^2) while the uncoated steel obtained a resistance of 2.11×10^5 (Ω cm^2), showing an increase of 64% and lower corrosion ratio (in mm/year) compared with the bare steel (from 3.50×10^{-3} to 1.85×10^{-3}), achieving a 47% reduction in the values obtained from the coated sample. A bare and covered area was observed in the samples after 24 h of immersion in NaCl, showing imperfections, pitting and concentrations in the bare zone. In contrast, the coated area presented little imperfection and selective concentrations of NaCl.

Acknowledgment

This work was supported by PRODEP2015-2018(Program for Professional Development Teacher, México), project number UANL-CA-378.

References

[1] J. P. Zamorano, L. A. T. Gonzalez, “Single technological innovation model in the automotive industry to eliminate rust conditions on metallic parts using nanomaterials”, Entretextos, Vol. 8, 2016, pp. 65–74.

[2] G. Hays, “Now is the time”, World Corros. Organ. 2018, http://corrosion.org/wco_media/nowisthetime.pdf, (accessed May 3, 2018).

[3] C. Soto. “Stainless steel corrosion study AISI 316 in chloride solutions”, Thesis, Universidad de Chile, Santiago de Chile, 2013.

[4] A. Shanaghi, A. R. Sabour, T. Shahrabi, M. Aliofkhazraee, “Corrosion protection of mild steel by applying TiO2 nanoparticle coating via sol-gel method”, Prot. Met. Phys. Chem. Surfaces, Vol. 45, No. 3, 2009, pp. 305–311.

[5] A. Shanaghi, A. S. Rouhaghdam, T. Shahrabi, M. Aliofkhazraei, “Study of TiO2 nanoparticle coatings by the sol-gel method for corrosion protection”, Mater. Sci., Vol. 44, No. 2, 2008, pp. 233–247.

[6] G. X. Shen, Y. C. Chen, C. J. Lin, “Corrosion protection of 316 L stainless steel by a TiO2

nanoparticle coating prepared by sol–gel method", Thin Solid Films, Vol. 489, No. 1, 2005, pp. 130–136.

[7] E. Mendoza, C. García, "Sol-gel coatings deposited on stainless steels alloys review", Rev. Dyna, Vol 74, 2007, pp. 101–110.

[8] B. Shayegh, "Design and Investigation of TiO2 –SiO2 Thin Films on AISI 316L Stainless", J. Adv. Mater. Process, Vol. 3, No. 3, 2015, pp. 13–24.

[9] M. Gobra, "Effects of TiO2/SiO2 reinforced nanoparticles on the mechanical properties of green hybrid coating", Int. Lett. Chem. Phys. Astron., 2015, pp. 56-66.

[10] W. C. Oliver, G. M. Pharr, "Measurement of hardness and elastic modulus by instrumented indentation: Advances in understanding and refinements to methodology", J. Mater. Res., Vol. 19, No. 1, 2004, pp. 3–20.

[11] S. R. Kalidindi, S. Pathak, "Determination of the effective zero-point and the extraction of spherical nanoindentation stress-strain curves", Acta Mater., Vol. 56, No. 14, 2008, pp. 3523–3532.

[12] O. I. Sekunowo, S. O. Adeosun, G. I. Lawal, "Potentiostatic Polarisation Responses Of Mild Steel In Seawater And Acid Environments", Int. J. Sci. Technol. Res., Vol. 2, No.10, 2013, pp. 139–145.

[13] M. F. Arenas, R. G. Reddy, "Corrosion of steel in ionic liquids", J. Min. Metall. J. Min. Met., No. 39, 2003, pp. 81–91.

[14] J. H. B. Ruíz, G. P. Rodríguez, "Effect of the number of layers in the coating surface properties of Si/Ti/Zr obtained from sol-gel suspensions", Rev. Cient. Guillermo Ockham, Vol. 8, No. 2, 2010, pp. 141–148.

[15] J. Krzak-Roś, J. Filipiak, C. Pezowicz, A. Baszczuk, M. Miller, M. Kowalski, R. Bedziński, "The effect of substrate roughness on the surface structure of TiO(2), SiO(2), and doped thin films prepared by the sol-gel method", Acta Bioeng. Biomech., Vol. 11, No. 2, 2009, pp. 21–29.

[16] D. Wang, G. P. Bierwagen, "Sol– gel coatings on metals for corrosion protection", Prog. Org. Coatings, Vol. 64, No. 4, 2009, pp. 327–338.

[17] S. M. Hosseinalipour, A. Ershad-langroudi, A. N. Hayati, A. M. Nabizade-Haghighi, "Characterization of sol-gel coated 316L stainless steel for biomedical applications", Prog. Org. Coatings, Vol. 67, No. 4, 2010, pp. 371–374.

[18] G. M. Pharr, W. C. Oliver, "Measurement of Thin Film Mechanical Properties Using Nanoindentation", MRS Bull., Vol. 17, No. 7, 1992, pp. 28–33.

[19] R. Lucchini, "Modelización de un ensayo de nanoindentación de capa fina de ZrW", Thesis, Universidad Politecnica de Catalunya, Catalunya, 2009.

[20] A. Bolshakov, G. M. Pharr, "Influences of pileup on the measurement of mechanical properties by load and depth sensing indentation techniques", J. Mater. Res., Vol. 13, No. 4, 1998, pp. 1049–1058.

[21] C. Geng, L. Fang, T. Wenwei, H. Zhenyu, C. Qingxin, "Experimental Report on the Nano-identation Testing of Textured Stainless Steel 904 L and 316 L", Procedia Eng., No. 99, 2015, pp. 1268–1274.

[22] J. Ballarre, E. Jimenez-Pique, M. Anglada, S. A. Pellice, A. L. Cavalieri, "Mechanical characterization of nano-reinforced silica based sol-gel hybrid coatings on AISI 316L stainless steel using nanoindentation techniques", Surf. Coatings Technol., Vol. 203, No. 20, 2009, pp. 3325–3331.

[23] Milton Ohring, "Materials Science of thin films Deposition and Structure", Academic Press, Second edition, London, UK, 2002, pp. 718-720.

[24] Sebahattin Kirtay, Characterization of SiO_2-TiO_2 Hybrid Corrosion Protective, Journal of Materials Engineering and Performance,vol. 23, nº 12, 2014,pp. 4309-4315.

[25] J. Uruchurtu Chavarin, J. Ramirez, "Experimental Methods in the Science of Corrosion Electrochemical Impedan (Métodos Experimentales en la Ciencia de la Corrosión Impedancia Electroquímica)", EAE Editorial Academia Española, 2016, pp. 54.